Radiative properties of numerically generated fractal soot aggregates : the importance of configuration averaging

Liu, Fengshan; Smallwood, Gregory J.

Publisher's version / Version de l'éditeur:
http://dx.doi.org/10.1115/1.4000245
Journal of heat transfer, 132, 2, 2010

Radiative Properties of Numerically Generated Fractal Soot Aggregates: The Importance of Configuration Averaging

Fengshan Liu

Gregory J. Smallwood

Institute for Chemical Process and Environmental Technology,
National Research Council,
Building M-9,
1200 Montreal Road,
Ottawa, ON, K1A 0R6, Canada

The radiative properties of numerically generated fractal soot aggregates were studied using the numerically accurate generalized multisphere Mie-solution method. The fractal aggregates investigated in this study contain 10–600 primary particles of 30 nm in diameter. These fractal aggregates were numerically generated using a combination of the particle-cluster and cluster-cluster aggregation algorithms with fractal parameters representing flame-generated soot. Ten different realizations were obtained for a given aggregate size measured by the number of primary particles. The wavelength considered is 532 nm, and the corresponding size parameter of primary particle is 0.177. Attention is paid to the effect of different realizations of a fractal aggregate with identical fractal dimension, prefactor, primary particle diameter, and the number of primary particles on its orientation-averaged radiative properties. Most properties of practical interest exhibit relatively small variation with aggregate realization. However, other scattering properties, especially the vertical-horizontal differential scattering cross section, are very sensitive to the variation in geometrical configuration of primary particles. Orientation-averaged radiative properties of a single aggregate realization are not always sufficient to represent the properties of random-oriented ensemble of fractal aggregates.
[DOI: 10.1115/1.4000245]

Keywords: fractal aggregates, soot, optical properties, configuration averaging

1 Introduction

The absorption and scattering properties of combustion-generated soot are required in many applications related to combustion and heat transfer. It is important to know the radiative properties of soot to quantify its contribution to thermal radiation transfer in flames, fires, and combustion systems. The radiative properties of soot are also essential in many optically based diagnostic techniques for quantitative measurements of soot properties, such as volume fraction and morphology (primary particle diameter and aggregate size). For example, the absorption cross section of soot aggregates is required to calculate the laser energy absorption rate and the thermal radiation intensity in laser-induced incandescence (LII) techniques when the effect of soot particle aggregation is taken into account [1,2] and the scattering properties of soot are required in multi-angle laser elastic scattering techniques for soot morphology measurements [3,4].

It has been established through thermophoretic sampling and subsequent transmission electron microscopy analysis that combustion-generated primary soot particle diameters fall in the range 10–60 nm for most combustion sources and, thus, can be reasonably assumed to be in the Rayleigh regime for the visible spectrum. It is also well known that soot forms aggregates containing nearly spherical primary particles [5,6]. Within any given aggregate, the sizes of the primary particle have a narrow distribution and can be approximately treated as identical in diameter [6]. Although there is a small degree of overlapping, bridging, or necking between two neighboring primary particles, it is reasonable to assume that primary particles are in point-contact [6]. This is an assumption commonly made in almost all theoretical and numerical studies of the optical properties of soot aggregates. Under these assumptions, the structure of soot aggregates can be described as mass fractal [5]. Due to such rather complex structure of soot aggregates, their optical properties cannot be adequately described by the Rayleigh approximation or the Mie-solution for the volume based equivalent sphere [7,8], since the rather open structure of soot aggregates cannot be represented by a compact sphere.

Various approximate methods have been developed and applied to calculate the radiative properties of fractal soot aggregates, such as the Rayleigh–Debye–Gans (RDG) theory [9], the discrete-dipole approximation [10], and the coupled electric and magnetic dipole (CEMD) method [11]. Although these methods are in general computationally efficient, especially the RDG theory, they can produce very inaccurate results under certain conditions. Two numerically accurate methods have been recently developed to predict the radiative properties of aggregates formed by nonoverlapping spherical particles: the cluster *T*-matrix method (CTM) [12,13] and the generalized multisphere Mie-solution (GMM) [14,15]. Executions of these numerically accurate methods require the position, diameter, and refractive index of each constituent sphere (primary particle). Although CTM has become the most popular method to study the radiative properties of various scatters [16–20], GMM has also been demonstrated to be a powerful tool to study the radiative properties of various particles [14,15,21,22]. In fact, CMT and GMM share a very similar theoretical framework, though differences exist [23]. However, GMM offers some advantages over CTM as discussed by Xu and Khlebtsov [23].

To represent the radiative properties of randomly oriented aggregates of a large population two kinds of averaging have been used [16]: one is the orientation averaging and the other is configuration or realization averaging. In the orientation averaging radiative properties are calculated for many different incident di-

Contributed by the Heat Transfer Division of ASME for publication in the JOURNAL OF HEAT TRANSFER. Manuscript received December 1, 2008; final manuscript received February 26, 2009; published online December 9, 2009. Assoc. Editor: Yogesh Jaluria.

rections for a single aggregate, and the results of all the orientations are averaged. In the latter, however, radiative properties are calculated for many different aggregates of identical morphological parameters at a fixed incident direction, and the results are averaged over all the configurations. A common assumption made in such practice is that orientation-averaged radiative properties of a single fractal aggregate can be used to represent those of an ensemble of random aggregates of identical morphological parameters (fractal dimension, prefactor, primary particle diameter, and number of primary particle) and optical properties (refractive index). Although this assumption seems reasonable based on the fact that the identical morphology parameters imply any fractal aggregate in this ensemble obey the same fractal scaling law and have the same radius of gyration, it is nevertheless questionable if one considers another fact that there are endless possibilities to generate a fractal aggregate of identical morphological parameters; i.e., the arrangement of individual constituent particles within the aggregate can still be random under the constraint that the fractal scaling law is satisfied.

This assumption has been recently investigated by Kolokolova et al. [17] and Liu and Mishchenko [19] using CTM. In the study of Kolokolova et al. [17], aggregates were numerically constructed using ballistic particle-cluster and cluster-cluster aggregation procedures [24,25]. Although it was not explicitly indicated in the study of Kolokolova et al. [17], these aggregates are indeed fractal, with a fractal dimension between 1.75 and 2.0 for cluster-cluster aggregation and about 2.45 for particle-cluster aggregation [25]. Moreover, Kolokolova et al. [17] did not mention the fractal dimensions for the aggregates they investigated. They investigated fractal aggregates containing 16 up to 128 primary particles and different primary particle size parameters in the range between 0.125 and 1.25. CTM calculations were conducted for only three different aggregate configurations for each set of morphological parameters. Their results showed that there are negligible variations in the absorption efficiency and the linear polarization with aggregate configuration; however, significant variations exist in the scattering efficiency, asymmetry factor, and scattering intensity, especially for smaller aggregates. In addition, that also found that the circular polarization is very sensitive to the arrangement of primary particles in an aggregate. For these reasons Kolokolova et al. [17] concluded that the orientation-averaged radiative properties of aggregates of the same structure and size often cannot represent those of an ensemble of such aggregates due to the influence of different arrangements of primary particles within the aggregate. They also recommended conducting both orientation and configuration averaging to obtain the correct results.

Liu and Mishchenko [19] studied the effect of aggregate realization (configuration) on orientation-averaged radiative properties of soot aggregates using the same solution method (CTM) as Kolokolova et al. [17], but a different method to numerically generate the fractal aggregates. In their study 20 different fractal aggregates containing 400 primary particles were generated using the algorithm described by Mackowski [26] along with morphological parameters typical of soot. Ensemble (realization) averaging of the orientation-averaged radiative properties was then carried out over the 20 realizations. The results of Liu and Mishchenko [19] showed that the standard deviations of scattering and absorption cross sections, the single-scattering albedo, and the asymmetry parameter are all within 3.5% of their corresponding mean. On the other hand, the relative differences in the scattering matrix elements are much larger but still within 15%. Based on these results, Liu and Mishchenko [19] concluded that the radiative properties obtained for one realization of a soot aggregate can be used to represent those of the entire ensemble of clusters having the same morphological parameters. Although Van-Hulle et al. [21] also investigated the effect of aggregate realization on the radiative properties of fractal soot aggregates, their results are not useful for examining the assumption mentioned above for the reason that the fractal aggregates they generated exhibit large variations in radius of gyration.

It is somewhat surprising to observe that Kolokolova et al. [17] and Liu and Mishchenko [19] reached opposite conclusions with regard to the importance of configuration or realization averaging to the radiative properties of a random-oriented ensemble of fractal aggregates. The present study is motivated by these contradictory findings. In this study, fractal soot aggregates containing 10–600 identical primary particles of 30 nm in diameter were numerically generated using a combined cluster-particle aggregation and cluster-cluster aggregation algorithm for specified fractal parameters (fractal dimension and prefactor). The resultant aggregates of different sizes have identical fractal parameters. Numerical calculations were conducted using GMM [14,15]. We attempt to conduct a similar study as that by Kolokolova et al. [17] and Liu and Mishchenko [19] to provide further numerical evidence to help answer the question if configuration averaging is necessary to predict the radiative properties of a random-oriented ensemble of aggregates.

2 Methodology

2.1 Numerical Generation of Fractal Aggregates. Soot, like many other fractal objects, is formed by the aggregation of small, nearly identical, and spherical primary particles into complex geometries. The fractal-like structure of soot aggregates obeys the following statistical scaling law [27]:

$$N = k_f \left(\frac{R_g}{a} \right)^{D_f} \tag{1}$$

where N is the number of primary particles within the aggregate, k_f and D_f are the prefactor and fractal dimension, respectively, a is the primary particle radius, and R_g is the radius of gyration defined as [28]

$$R_g^{\,2} = \frac{1}{N} \sum_{i=1}^{N} (\mathbf{r}_i - \mathbf{r}^0)^2 + a^2 \tag{2}$$

$$\mathbf{r}^0 = \frac{1}{N} \sum_{i=1}^{N} \mathbf{r}_i \tag{3}$$

where vectors $\mathbf{r}_i$ and $\mathbf{r}^0$ define the position of the center of the ith primary particle and the center of the aggregate, respectively. For the current study, fractal aggregates simulating flame-generated soot were numerically generated using the particle-cluster aggregation algorithm for small aggregates (up to $N=31$) and cluster-cluster aggregation algorithm for larger aggregates. The algorithms used in this study follow closely those described by Filippov et al. [28], and the details of our numerical implementation of these algorithms can be found in Ref. [22]. It is worth noting that the algorithms for the generation of numerical fractal aggregates in this study are also very similar to those used by Liu and Mishchenko [19]. As demonstrated by Filippov et al. [28], the density correlation functions of fractal aggregates generated by the cluster-cluster aggregation algorithm give the correct slope when plotted against the nondimensional distance on a log-log scale. The following morphological parameters were used in the generation of fractal aggregates: $k_f=2.3$, $D_f=1.78$, and $a=15$ nm, which are typical values for flame-generated soot. Fractal aggregates containing $N=10$, 20, 50, 100, 200, 400, and 600 primary particles were generated using this combined particle-cluster and cluster-cluster aggregation algorithm. For all the aggregate sizes except $N=200$, ten different realizations were generated. In the case of $N=200$, 30 different aggregates were constructed.

To demonstrate the variability in the arrangement of primary particles in aggregates of identical morphology, the first six aggre-

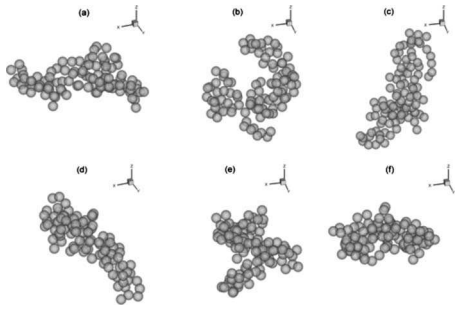

Fig. 1 The first six realizations for $N=100$

gate realizations for $N=100$ are displayed in Fig. 1. It is evident that the aggregates can have very different arrangements of individual primary particles. It is recognized that these aggregates are somewhat more compact than typical soot aggregates. This is because a somewhat large value of the prefactor $k_f=2.3$ is used.

2.2 Generalized Multisphere Mie-Solution. In this study GMM was used to calculate the orientation-averaged radiative properties of the numerically generated fractal aggregates. Similar to CTM, GMM is also numerically exact and much more efficient than the other numerical techniques based on an explicit solution of the Maxwell equations. GMM was developed by Xu [14,15] based on the framework of the Mie theory for a single sphere and the addition theorems for spherical vector wave functions. GMM provides a rigorous and complete solution to nonoverlapping multisphere light scattering problems and can be readily applied to fractal aggregates [21,22]. The key steps involved in the development of GMM include (a) expansion of the scattered, internal, and incident electromagnetic fields in terms of vector spherical functions; (b) formation of a linear equation system through the boundary condition at each primary particle in the aggregate; (c) transformation of the waves scattered by an individual primary particle into the incident waves of the other particles in the aggregate through the addition theorems for vector spherical functions; and (d) solution of the linear system of interactive coefficients. The absorption and scattering cross sections and the four scattering matrix coefficients are analytically given by Xu [14,15]. GMM rigorously accounts for the multiple scattering within the aggregate. However, GMM is still very computationally demanding and memory intensive for large aggregates containing several hundred primary particles, especially when the size parameter of the primary particle is relatively large.

3 Results and Discussion

Numerical calculations were conducted for 532 nm wavelength, which is of great interest in laser scattering and LII experiments. The corresponding primary particle size parameter is $x_p=\pi d_p/\lambda$, and is relatively small at 0.177. The refractive index of soot was assumed to be $m=1.6+0.6i$, which is again a typical value of soot in the visible spectrum. Orientation averaging was achieved numerically in the GMM calculations by dividing each Euler angle into 15 equal-intervals. Although the apparent number of orientations considered is 3375, the actual number of orientations to be calculated is doubled by selecting the feature of IDD=1 [29]. Such level of orientation averaging is considered sufficient based on previous studies [16]; i.e., further division of the three Euler angles would not affect the orientation-averaged results.

3.1 Absorption and Total Scattering Cross Sections and Asymmetry Parameter. The ensemble-averaged cross sections of absorption and total scattering and the asymmetry parameter were calculated using the following expressions [19]:

Table 1 Configuration-averaged absorption and total scattering cross sections and asymmetry parameter and their maximum relative deviations for orientation- and realization-averaged results, based on ten realizations unless otherwise noted

N	C_{abs} (nm^2)	Maximum ε in C_{abs} (%)	C_{sca} (nm^2)	Maximum ε in C_{sca} (%)	g	Maximum ε in g (%)
10	1,508.9	0.63	43.0	0.05	0.0481	3.69
20	3,046.5	1.31	154.2	1.04	0.0979	1.69
50	7,596.3	0.37	675.9	2.06	0.254	5.36
100	15,012.0	0.63	1,769.2	4.51	0.417	7.12
200	29,572.1	0.28	4,330.9	3.92	0.529	5.13
200[a]	29,559.0	0.60	4,312.8	4.36	0.533	6.54
200[b]	29,551.9	0.58	4,312.4	4.37	0.536	6.46
400	58,097.1	0.50	10,004.6	2.68	0.621	7.28
600	86,387.7	0.53	16,182.5	5.29	0.656	4.22

[a]Based on 20 realizations.
[b]Based on 30 realizations.

$$C_{abs}=\frac{1}{M}\sum_{i=1}^{M} C_{abs}{}^{i} \tag{4}$$

$$C_{sca}=\frac{1}{M}\sum_{i=1}^{M} C_{sca}{}^{i} \tag{5}$$

$$g=\frac{1}{MC_{sca}}\sum_{i=1}^{M} g^{i}C_{sca}{}^{i} \tag{6}$$

where subscripts abs and sca represent absorption and scattering, respectively, and superscript i denotes orientation-averaged quantities of the ith aggregate realization. The numerical results of the absorption and total scattering cross sections and the asymmetry parameter are summarized in Table 1. In this table, the relative deviation ε is defined as $|X^{i}-X_{mean}|/X_{mean}\times 100\%$ (X is either C_{abs}, C_{sca}, or g). It is evident that the absorption cross section varies negligibly with aggregate realization for all the aggregate sizes considered. Although the total scattering cross section and the asymmetry parameter exhibit larger variations with the aggregate realization than the absorption cross section, the relative deviations are still considered small as they remain less than 7.5%. Kolokolova et al. [17] reported that there are significant relative deviations in C_{sca} and g (about 15%) with aggregate realization for $N=16$ and $x_p=0.125$, which are comparable to the present conditions of $N=20$ and $x_p=0.177$. Unlike the results of Kolokolova et al. [17] for $N=16$ and $x_p=0.125$, however, our results of C_{sca} and g for $N=20$ and $x_p=0.177$ do not display large variations with aggregate realization. The relative deviations in C_{sca} and g for larger aggregates are similar but smaller to those reported by Kolokolova et al. [17]. The maximum relative deviations in C_{sca} and g are also comparable to the relative errors in C_{sca} and g of Liu and Mishchenko [19] measured by the ratio of standard deviation to mean.

The results for $N=200$ and different realizations indicate that 20 realizations seem sufficient to achieve converged results; however, 10 realizations can be considered as adequate. Nevertheless, the results shown in Table 1 suggest that the aggregate realization or configuration, i.e., the detailed arrangement of individual primary particles within the aggregate, has almost no influence on the orientation-averaged absorption cross section, and only small or modest impact on the total scattering cross section and the asymmetry parameter.

The present normalized averaged absorption and total scattering cross sections over both orientation and aggregate realization for a given aggregate size are compared with the results of RDG and

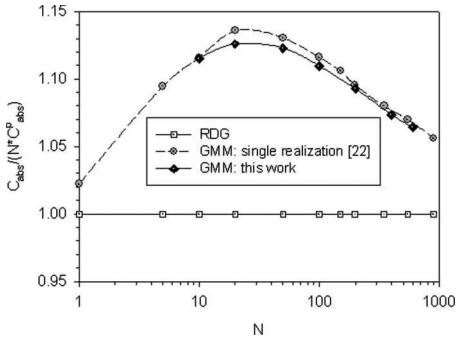

Fig. 2 Comparison of nondimensional aggregate absorption cross section

our previous GMM for a single aggregate realization using the same fractal parameters and soot refractive index [22] in Figs. 2 and 3, respectively. The superscript p indicates quantities of the primary particle in the Rayleigh limit. It is evident from these figures that the effect of realization averaging is quite small, consistent with the results displayed in Table 1. Nevertheless, realization averaging results in a smoother distribution of C_{abs}. The deviation of the RDG results from those of GMM or other more accurate solutions is well known, especially for the absorption cross section. These results indicate that it is adequate to perform GMM calculations for the absorption and total scattering cross sections and the asymmetry parameter of an ensemble of random-oriented fractal aggregates using just a single realization. In this regard, the present finding agrees with that made by Liu and Mishchenko [19]. This conclusion has significant implications in practice, since it means not only that previous results of the optical properties of fractal aggregates based on a single realization are valid but also huge computing efforts can be avoided in future studies.

3.2 Differential Scattering Cross Sections. The nondimensional differential scattering cross sections k^2C_{VV} for different realizations of $N=100$ and 400 are compared in Fig. 4; here $k=2\pi/\lambda$ is the wavenumber, the first subscript in C_{VV} refers to the incident polarization, and the second to the detected polarization. The following observations can be made from the results shown in this figure. First, the differential cross section C_{VV} in the near forward directions is almost independent of the aggregate realization. However, the angular range for such independence becomes narrower as the aggregates become larger. Second, the differential cross section C_{VV} displays a relatively large sensitivity to the aggregate realization at large scattering angles, i.e., in the backward directions. These results indicate the increasing importance of aggregate realization (arrangement of primary particles) as the scattering angle increases. A similar observation of such behavior

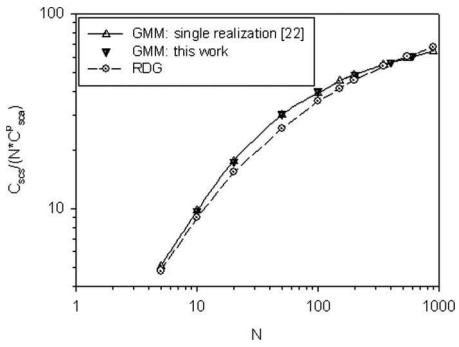

Fig. 3 Comparison of nondimensional aggregate total scattering cross section

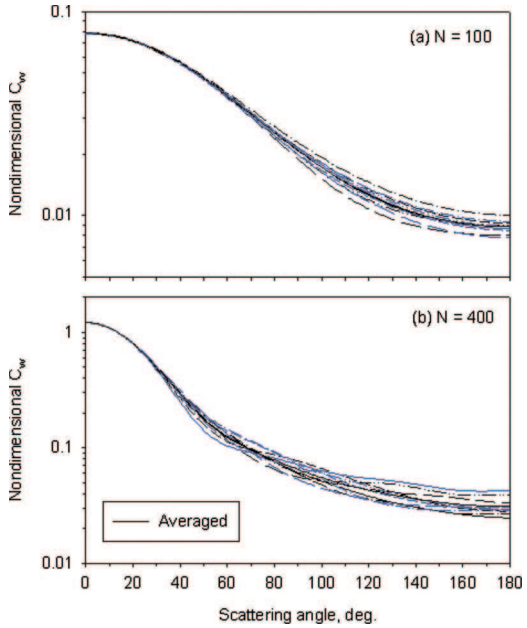

Fig. 4 Nondimensional vertical-vertical differential scattering cross sections for different aggregate realizations and $N=100$ and 400

of C_{VV} has been made previously by Farias et al. [30]. The results of horizontal-horizontal differential scattering cross section C_{HH} have a similar dependence on aggregate realization to C_{VV} and can be found in Ref. [22]. Therefore, the results of C_{HH} are not shown.

The scattering phase function is related to the scattering cross sections as

$$\Phi(\theta)=\frac{4\pi}{C_{sca}}\frac{(C_{VV}+C_{HH})}{2} \tag{7}$$

The effects of aggregate realization on the scattering phase function for $N=100$ and 400 are shown in Fig. 5. In the calculation of the configuration-averaged phase function, the configuration-averaged total and differential scattering cross sections are used in Eq. (7). The scattering quickly becomes primarily in the forward direction as the aggregate size increases. The effect of aggregate realization is relatively small with deviations comparable to those for the total scattering cross section and the asymmetry parameter given in Table 1.

Although the results shown in Fig. 4 are a clear indication that the vertical-vertical differential scattering cross section is somewhat sensitive to the detailed arrangement of primary particles, C_{VV} is not the best quantity to demonstrate the importance of aggregate realization. This is because C_{VV} is dominated by single scattering [31], and a better way to reveal the importance of primary particle arrangement is to examine the quantities dominated by multiple scattering. Such quantities include the circular polarization [17] and depolarization [31,32]. It is well known that the presence of depolarization is an indication of multiple scattering. Here we examine depolarization quantified by the differential scattering cross section C_{VH} at the forward direction, i.e., at scattering angle $\theta=0$ deg. The results of orientation-averaged $C_{VH}(0 \text{ deg})$ for different aggregate realizations and different N are summarized in Table 2. It is evident that $C_{VH}(0 \text{ deg})$ is sensitive to aggregate realization and the relative variation can vary by more than a factor of 4. For this reason, our results support the conclusion reached by Kolokolova et al. [17] that it is important to perform configuration averaging to obtain correct complete radiative properties of random-oriented ensemble of fractal aggregates.

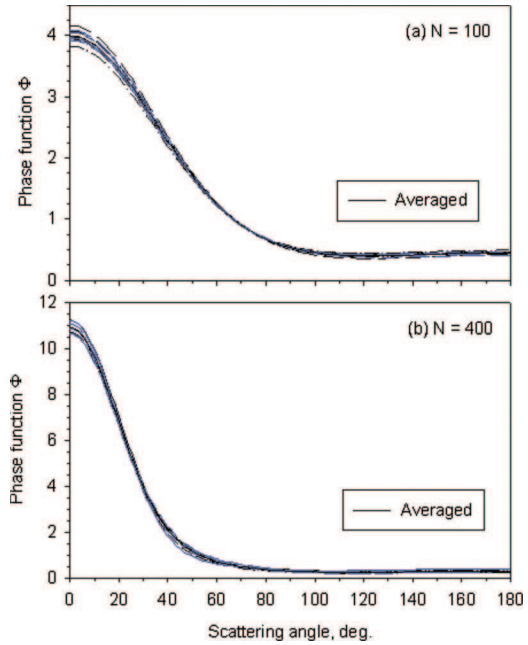

Fig. 5 Scattering phase functions for different aggregate realizations and $N=100$ and 400

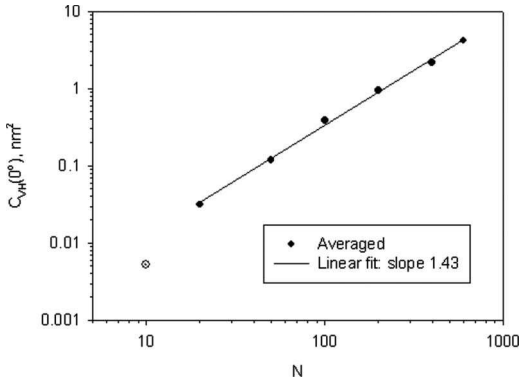

Fig. 6 Variation of configuration- and orientation-averaged C_{VH}(0 deg) with aggregate size N

Chen et al. [33] showed that second-order light scattering (SOLS) (C_{VH} is a special case of SOLS) is sensitive to the structural anisotropy of a cluster, which is determined by the arrangement of primary particles. It is clear that the radiative properties of fractal aggregates that are dominated by multiple scattering and sensitive to the specific arrangement of primary particles require a certain tool to describe the subtle difference from one aggregate to the other among aggregates of identical morphology dictated by k_f, D_f, a, and N. Such subtle difference has been discussed by Seeley et al. [34] in terms of higher-order geometry of such fractal aggregates. The results shown in Table 2 clearly indicate that the orientation-averaged differential scattering cross section C_{VH} calculated from a particular aggregate realization cannot be used to represent that of a random-oriented ensemble of aggregates.

Because of the large variation of C_{VH}(0 deg) from one realization to another, the adequacy of using only ten realizations for obtaining its configuration-averaged value is somewhat questionable. Nevertheless, variation of the configuration- and orientation-averaged C_{VH}(0 deg) with aggregate size N is plotted in Fig. 6 in a log-log scale, since it is expected that C_{VH} is proportional to N^x [33]. Except for the point at the smallest aggregate size considered ($N=10$), there exists a very good linear fit with a slope of 1.43, which is close to the value of 1.5 obtained by Chen et al. [33] for bond-percolation clusters. The good linear fit implies that it is reasonable to use ten realizations for configuration averaging of C_{VH}(0 deg). If the point at $N=10$ were included in the linear fit, a higher slope of 1.56 was obtained with a much worse fit quality.

4 Conclusion

The effect of configuration averaging on the radiative properties of soot fractal aggregates was investigated using the generalized multisphere Mie-solution method along with a combined particle-cluster and cluster-cluster aggregation algorithm for generating fractal aggregates of identical morphology. The present results show that the orientation-averaged absorption and total scattering cross sections and the asymmetry parameter exhibit relatively small variation from one realization to the other with a maximum relative deviation of less than about 7%, especially for the absorption cross section with a maximum relative deviation of about 1%. Such effects of aggregate realization are similar to some previous findings. Therefore, we can conclude that it is reasonable to conduct numerical calculations using just one aggregate realization to represent orientation-averaged absorption and total scattering cross sections, the asymmetry parameter, the scattering phase function, and the vertical-vertical and horizontal-horizontal differential scattering cross sections of an ensemble of random-oriented soot fractal aggregates. The present configuration- and orientation-averaged absorption and total scattering cross sections are in good agreement with our previous results obtained for a single aggregate realization.

The arrangement of primary particles in aggregates of identical morphological parameters has modest impact on the vertical-vertical differential scattering cross section at larger scattering angles. The quantities dominated by multiple scattering, such as the vertical-horizontal differential scattering cross section, display

Table 2 Orientation-averaged C_{VH}(0 deg) (in nm^2) for different aggregate realizations and different aggregate sizes N

	$N=10$	$N=20$	$N=50$	$N=100$	$N=200$	$N=400$	$N=600$
1	3.70×10^{-3}	4.22×10^{-2}	0.181	0.425	0.782	3.968	8.083
2	7.57×10^{-3}	1.80×10^{-2}	0.145	0.656	1.659	4.287	6.219
3	3.66×10^{-3}	5.62×10^{-2}	0.104	0.159	0.793	1.323	3.624
4	3.30×10^{-3}	3.88×10^{-2}	0.139	0.518	1.818	1.613	6.266
5	3.51×10^{-3}	2.26×10^{-2}	0.146	0.290	0.584	0.398	1.473
6	5.91×10^{-3}	4.27×10^{-2}	0.0897	0.480	0.990	2.477	4.201
7	7.63×10^{-3}	2.97×10^{-2}	0.0543	0.0778	0.294	0.961	2.545
8	1.03×10^{-3}	1.37×10^{-2}	0.123	0.312	0.571	4.112	5.140
9	4.35×10^{-3}	3.81×10^{-2}	0.091	0.304	0.937	0.803	2.276
10	2.40×10^{-3}	1.13×10^{-2}	0.102	0.629	1.115	1.807	2.043
Averaged	5.23×10^{-3}	3.13×10^{-2}	0.118	0.385	0.954	2.175	4.187

a much higher sensitivity to aggregate realization. For this reason, it is concluded that a single aggregate realization cannot be used to represent the radiative properties of a random-oriented ensemble of aggregates as far as the vertical-horizontal differential scattering cross section is concerned. This finding is likely applicable to other quantities related to the asymmetric structure of fractal aggregates, but further investigation is required. The configuration- and orientation-averaged vertical-horizontal differential scattering cross sections of the soot aggregates investigated increase with the aggregate size as $N^{1.43}$.

Acknowledgment

We would like to thank Dr. Y.-L. Xu for making his GMM computer codes available. Financial support was provided in part by the Government of Canada's PERD Program through Project Nos. C23.006 and C11.003.

Nomenclature

a = radius of primary particle, nm
C = cross section area, nm^2
D_f = fractal dimension
g = asymmetry parameter
k = wavenumber
k_f = fractal prefactor
m = refractive index
N = number of primary particles in aggregate
$\mathbf{r}$ = center of primary particle
$\mathbf{r}^0$ = center of aggregate
R_g = radius of gyration, nm
x_p = size parameter of primary particle

Greek Symbols

λ = wavelength, nm
θ = scattering angle, deg
Φ = scattering phase function

Subscripts

abs = absorption
H = horizontally polarized
sca = total scattering
V = vertically polarized

References

[1] Snelling, D. R., Liu, F., Smallwood, G. J., and Gülder, Ö. L., 2004, "Determination of the Soot Absorption Function and Thermal Accommodation Coefficient Using Low-Fluence LII in a Laminar Coflow Ethylene Diffusion Flame," Combust. Flame, **136**, pp. 180–190.
[2] Liu, F., Yang, M., Hill, F. A., Snelling, G. J., and Smallwood, G. J., 2006, "Influence of Polydisperse Distributions of Both Primary Particle and Aggregate Size on Soot Temperature in Low-Fluence LII," Appl. Phys. B: Lasers Opt., **83**, pp. 383–395.
[3] Köylü, Ü. Ö., 1997, "Quantitative Analysis of In Situ Optical Diagnostics for Inferring Particle/Aggregate Parameters in Flames: Implications for Soot Surface Growth and Total Emissivity," Combust. Flame, **109**, pp. 488–500.
[4] Yang, B., and Köylü, Ü. Ö., 2005, "Soot Processes in a Strongly Radiating Turbulent Flame From Laser Scattering/Extinction Experiments," J. Quant. Spectr. Rad. Trans., **93**, pp. 289–299.
[5] Megaridis, C. M., and Dobbins, R. A., 1990, "Morphological Description of Flame-Generated Materials," Combust. Sci. Technol., **71**, pp. 95–109.
[6] Faeth, G. M., and Köylü, Ü. Ö., 1995, "Soot Morphology and Optical Properties in Nonpremixed Turbulent Flame Environments," Combust. Sci. Technol., **108**, pp. 207–229.
[7] Dalzell, W. H., Williams, G. C., and Hottel, H. C., 1970, "A Light-Scattering Method for Soot Concentration Measurements," Combust. Flame, **14**, pp. 161–170.
[8] Köylü, Ü. Ö., and Faeth, G. M., 1993, "Radiative Properties of Flame-Generated Soot," ASME J. Heat Transfer, **115**, pp. 409–417.
[9] Köylü, Ü. Ö., and Faeth, G. M., 1994, "Optical Properties of Overfire Soot in Buoyant Turbulent Diffusion Flames at Long Residence Time," ASME J. Heat Transfer, **116**, pp. 152–159.
[10] Draine, B. T., and Flatau, P. J., 1994, "Discrete-Dipole Approximation for Scattering Calculations," Opt. Soc. Am, **11**, pp. 1491–1499.
[11] Mulholland, G. W., Bohren, C. F., and Fuller, K. A., 1994, "Light Scattering by Agglomerates: Coupled Electric and Magnetic Dipole Method," Langmuir, **10**, pp. 2533–2546.
[12] Mishchenko, M. I., 1991, "Light Scattering by Randomly Oriented Axially Symmetric Particles," J. Opt. Soc. Am. A, **8**, pp. 871–882.
[13] Khlebtsov, N. G., 1992, "Orientational Averaging of Light-Scattering Observables in the T-Matrix Approach," Appl. Opt., **31**, pp. 5359–5365.
[14] Xu, Y.-L., 1995, "Electromagnetic Scattering by an Aggregate of Spheres," Appl. Opt., **34**, pp. 4573–4588.
[15] Xu, Y.-L., 1997, "Electromagnetic Scattering by an Aggregate of Spheres: Far Field," Appl. Opt., **36**, pp. 9496–9508.
[16] Riefler, N., di Stasio, S., and Wriedt, T., 2004, "Structural Analysis of Clusters Using Configurational and Orientational Averaging in Light Scattering Analysis," J. Quant. Spectr. Rad. Trans., **89**, pp. 323–342.
[17] Kolokolova, L., Kimura, H., Ziegler, K., and Mann, I., 2006, "Light-Scattering Properties of Random-Oriented Aggregates: Do They Represent the Properties of an Ensemble of Aggregates?," J. Quant. Spectr. Rad. Trans., **100**, pp. 199–206.
[18] Liu, L., and Mishchenko, M. I., 2005, "Effects of Aggregation on Scattering and Radiative Properties of Soot Aerosols," J. Geophys. Res., **110**, p. D11211.
[19] Liu, L., and Mishchenko, M. I., 2007, "Scattering and Radiative Properties of Complex Soot and Soot-Containing Aggregate Particles," J. Quant. Spectr. Rad. Trans., **106**, pp. 262–273.
[20] Mishchenko, M. I., Videen, G., Khlebtsov, G., Wriedt, T., and Zakharova, N. T., 2008, "Comprehensive T-Matrix Reference Database: A 2006-07 Update," J. Quant. Spectr. Rad. Trans., **109**, pp. 1447–1460.
[21] Van-Hulle, P., Weill, M.-E., Talbaut, M., and Coppalle, A., 2002, "Comparison of Numerical Studies Characterizing Optical Properties of Soot Aggregates for Improved EXSCA Measurements," Part. Part. Syst. Charact., **19**, pp. 47–57.
[22] Liu, F., and Snelling, D. R., 2008, "Evaluation of the Accuracy of the RDG Approximation for the Absorption and Scattering Properties of Fractal Aggregates of Flame-Generated Soot," Paper No. AIAA-2008-4362.
[23] Xu, Y.-L., and Khlebtsov, N. G., 2003, "Orientational-Averaged Radiative Properties of an Arbitrary Configuration of Scatters," J. Quant. Spectr. Rad. Trans., **79–80**, pp. 1121–1137.
[24] Meakin, P., 1983, "The Vold-Sutherland and Eden Models of Cluster Formation," J. Colloid Interface Sci., **96**, pp. 415–424.
[25] Meakin, P., 1984, "Effects of Cluster Trajectories on Cluster-Cluster Aggregation: A Comparison of Linear and Brownian Trajectories in Two- and Three-Dimensional Simulations," Phys. Rev. A, **29**, pp. 997–999.
[26] Mackowski, D. W., 2006, "A Simplified Model to Predict the Effects of Aggregation on the Absorption Properties of Soot Particles," J. Quant. Spectr. Rad. Trans., **100**, pp. 237–249.
[27] Forrest, S. R., and Witten, T. A., Jr., 1979, "Long-Range Correlations in Smoke-Particle Aggregates," J. Phys. A, **12**, pp. L109–L117.
[28] Filippov, A. V., Zurita, M., and Rosner, D. E., 2000, "Fractal-Like Aggregates: Relation Between Morphology and Physical Properties," J. Colloid Interface Sci., **229**, pp. 261–273.
[29] http://www.astro.ufl.edu/~xu/codes/gmm01f
[30] Farias, T. L., Carvalho, M. G., Köylü, Ü. Ö., and Faeth, G. M., 1995, "Computational Evaluation of Approximate Rayleigh-Debye-Gans/Fractal-Aggregate Theory for the Absorption and Scattering Properties of Soot," ASME J. Heat Transfer, **117**, pp. 152–159.
[31] Sorensen, C. M., 2001, "Light Scattering by Fractal Aggregates: A Review," Aerosol Sci. Technol., **35**, pp. 648–687.
[32] Lu, N., and Sorensen, C. M., 1994, "Depolarization Light Scattering From Fractal Soot Aggregates," Phys. Rev. E, **50**, pp. 3109–3115.
[33] Chen, Z.-Y., Weakliem, P., Gelbart, W. M., and Meakin, P., 1987, "Second-Order Light Scattering and Local Anisotropy of Diffusion-Limited Aggregates and Bond-Percolation Clusters," Phys. Rev. Lett., **58**, pp. 1996–1999.
[34] Seeley, G., Keyes, T., and Ohtsuki, T., 1988, "Higher-Order Fractal Geometry; Application to Multiple Light Scattering," Phys. Rev. Lett., **60**, pp. 290–293.